

# The XO planetary survey project — Astrophysical false positives

Radosław Poleski<sup>1</sup>, Peter R. McCullough<sup>2</sup>, Jeff A. Valenti<sup>2</sup>, Christopher J. Burke<sup>2</sup>, Pavel Machalek<sup>2,3</sup>, Kenneth Janes<sup>4</sup>  
rpoleski@astrouw.edu.pl

## ABSTRACT

Searches for planetary transits find many astrophysical false positives as a by-product. There are four main types analyzed in the literature: a grazing-incidence eclipsing binary star, an eclipsing binary star with a small radius companion star, a blend of one or more stars with an unrelated eclipsing binary star, and a physical triple star system. We present a list of 69 astrophysical false positives that had been identified as candidates of transiting planets of the on-going XO survey. This list may be useful in order to avoid redundant observation and characterization of these particular candidates independently identified by other wide-field searches for transiting planets. The list may be useful for those modeling the yield of the XO survey and surveys similar to it. Subsequent observations of some of the listed stars may improve mass-radius relations, especially for low-mass stars. From the candidates exhibiting eclipses, we report three new spectroscopic double-line binaries and give mass function estimations for 15 single lined spectroscopic binaries.

*Subject headings:* astronomical data bases: miscellaneous — binaries: eclipsing — binaries: spectroscopic — eclipses — ephemerides — surveys — techniques: radial velocities

## 1. Introduction

A planetary transit indicates that the orbital inclination  $i \approx 90^\circ$ , so the projection factor  $\sin(i)$  is near unity and thus measurements of the radial velocity (hereafter RV) of the star, which mass is known, reveal the true mass of the planet,  $M_p$ , not just the product  $M_p \sin(i)$ . Furthermore, the photometric depth of a transit indicates the ratio of the planetary radius to the stellar radius.

With increasing precision of the observations, planetary transits provide a wealth of information about the physical characteristics of the planet and the star (see e.g. Charbonneau

2007). Because of their importance, much effort has been applied to finding transiting planets and dozens have been reported.<sup>1</sup> The results described in this work originate from the XO project (McCullough et al. 2005), and because the characteristics of that survey are similar to other transit surveys such as HAT (Bakos et al. 2002), WASP (Pollacco et al. 2006), TrES (Dunham et al. 2004), some of the results may be helpful to avoid redundant observations for transit candidates selected by these surveys.

Planetary transit surveys produce a large number of homogeneous photometric measurements. Paczyński (2000) listed many ways in which data collected by massive photometric surveys can be used for astrophysical research. During planetary searches many objects mimicking planetary transits are discovered: eclipsing binaries (EB) on grazing incidence orbits, small stars transiting larger stars (e.g. an M dwarf plus an F

<sup>1</sup>University of Warsaw Observatory, Al. Ujazdowskie 4, 00-478 Warszawa, Poland

<sup>2</sup>Space Telescope Science Institute, 3700 San Martin Drive, Baltimore, MD 21218, USA

<sup>3</sup>Department of Physics and Astronomy, Johns Hopkins University, Baltimore, MD 21218, USA

<sup>4</sup>Astronomy Department, Boston University, 725 Commonwealth Avenue, Boston, MA 02215, USA

<sup>1</sup><http://www.inscience.ch/transits/>

dwarf or a dwarf and a giant) or eclipsing binary systems with the orbital periods between 0.5 d and 10 d (typical period search criteria) diluted by a bright star (either physically connected or not) which reduces the eclipse depth to approximately 1 %. In grazing-incidence case, the orbital period is two times longer than the photometric one and these systems can sometimes be distinguished if the odd and even eclipses have different depths, which implies different surface brightnesses, or the separation in time from one eclipse to the next is bimodal, which would imply an eclipsing binary in an eccentric orbit. It is sometimes extremely difficult to prove the true nature of transiting objects (see e.g. Hoyer et al. 2007). Creevey et al. (2005), Young et al. (2006) and Beatty et al. (2007) showed that follow up observations of these stellar transits can further our knowledge of the K and M dwarfs.

Transiting extrasolar planets are typically found by photometric surveys and later-on confirmed by RV observations. More often than not, the subsequent RV measurements reveal not a planet but an *astrophysical false positive* (Brown 2003). In this paper we report on some of the astrophysical false positives observed by the XO project (McCullough et al. 2005). The structure of the paper is as follows: §2 describes the photometric observations and their analysis, §3 describes the list of astrophysical false positives and compares it with other similar lists, §4 discusses the radial velocity measurements followed by discussion of selected objects in §5 and conclusions in §6.

## 2. Photometric observations and their analysis

McCullough et al. (2005) described the equipment and the observation strategy associated with the data analyzed here. Since September 2003 two XO cameras have operated autonomously at Haleakala summit in Hawaii. Each camera consists of a wide-field 200 mm f/1.8 lens combined with a 1024×1024 pixel CCD detector observing in the 0.4  $\mu\text{m}$  to 0.7  $\mu\text{m}$  band-pass. The field of view is  $7^\circ 2' \times 7^\circ 2'$ . Each pixel is 24  $\mu\text{m}$  yielding an image scale of  $25''/4$  per pixel. Both cameras are attached to the same German-equatorial mount, operating in a drift-scan mode along the N-S strips. Each

star is observed by both cameras every 10 minutes with 54 s exposures. On many nights, some stars are observed for less than 4 h so frequently only an ingress or an egress is observed. Up to 45000 stars brighter than 13.3 mag in *V* per strip are analyzed for planetary transits. The standard deviation of photometric time series for stars brighter than 12 mag is typically less than 10 mmag. Stars brighter than 8.5 mag are saturated and thus not analyzed.

Here we present an analysis of seven strips each  $7.2^\circ$  wide, covering declinations from  $0^\circ$  to  $63^\circ$  and centered at right ascensions 0, 4, 7.5, 8, 12, 15.5 and 16 hours. Since we observe each strip for  $\approx 4$  months each year, for some targets only a few transits are observed which leads to possible period ambiguities. In present study we have used data collected during: two and a half seasons for 0 and 4 h RA strip, one season for 15.5 h RA strip and two seasons for the rest of the strips.

Two different methods were employed to correct photometric data for systematic errors: SysRem (Tamuz et al. 2005) and one described by McCullough et al. (2005). Each of these methods produced one set of input data for planetary transit search, for which we used the Box-fitting Least Squares algorithm (BLS; see Kovács et al. 2002), as modified by McCullough et al. (2005). For the most promising candidates we combined BLS results (depth, period and duration of the transit) with catalog information to estimate the planetary radius and other ancillary facts related to the star.

Because of the large pixel scale of the XO cameras, there is a substantial possibility that a nearby bright star can contaminate the light from an EB, mimicking a planetary transit. Thus, for each candidate we calculated the fraction of light (hereafter FL75) within the XO photometric aperture ( $r = 75''$ ) from varying source using the 2MASS point-source catalog (Skrutskie et al. 2006). The estimate of FL75 gives possibility to better constrain undiluted transit depth:

$$\delta m_{FL75} = -2.5 \log \left( 1 - \frac{1 - 10^{-0.4\delta m}}{FL75} \right) \quad (1)$$

Where  $\delta m$  is transit depth found using BLS on XO data and  $\delta m_{FL75}$  is expected undiluted depth. At the beginning of selection process it is not known which of the stars situated within XO photometric aperture is varying and only lower limit on  $\delta m_{FL75}$

can be constrained. One should note that the true transit depth can differ from the XO one also because BLS fits a box-shaped function to the transit and in most cases BLS underestimates the depth.

One of the methods used for identification of blended double system involves centroid shift (McCullough & Burke 2007; Burke et al. 2006). For each candidate we compared astrometric positions measured during in-transit and out-of-transit observations. In this paper we present three candidates eliminated only using centroid shift. Standard deviations of mean positions were  $\approx 0''.03$  in almost all cases.

Follow-up photometric observations of selected candidates are conducted by the XO Extended Team (hereafter ET) with higher angular resolution and in several band-passes. The ET is composed of amateur astronomers whose observing sites are dispersed widely in longitude. Their observations often show blended neighbors of target stars. The ET observations also have higher photometric precision and better timing of transits which is useful for improving the accuracy of the ephemerides and identifying the nature of transiting planet candidates. Representative light curves from ET observations are shown in other papers (Burke et al. 2007, 2008; McCullough et al. 2006; Johns-Krull et al. 2008; Garcia-Melendo & McCullough 2009).

### 3. List of astrophysical false positives

Table 1 lists stars which passed automated selection criteria and showed variations similar to a planetary transits on the XO photometric data. We report there: 2MASS designation, the XO brightness ( $m_{XO}$ ), FL75, transit properties given by BLS (depth  $\delta m$ , duration  $t_{dur}$ , period  $P$  and time of epoch  $T_0$ ),  $\delta m_{FL75}$ , the type of the astrophysical false positive and additional remarks. Figure 1 shows exemplary light curves for astrophysical false positives.

The XO data presented here cover an area of  $3539 \text{ deg}^2$ , with 69 astrophysical false positives. The SuperWASP fields analyzed by Christian et al. (2006), Clarkson et al. (2007) and Kane et al. (2008) were  $1507 \text{ deg}^2$ ,  $786 \text{ deg}^2$  and  $2162 \text{ deg}^2$  with 41, 44 and 30 false positives, respectively. The common area with XO were equal to  $133 \text{ deg}^2$ ,  $188 \text{ deg}^2$  and  $361 \text{ deg}^2$ , respectively.

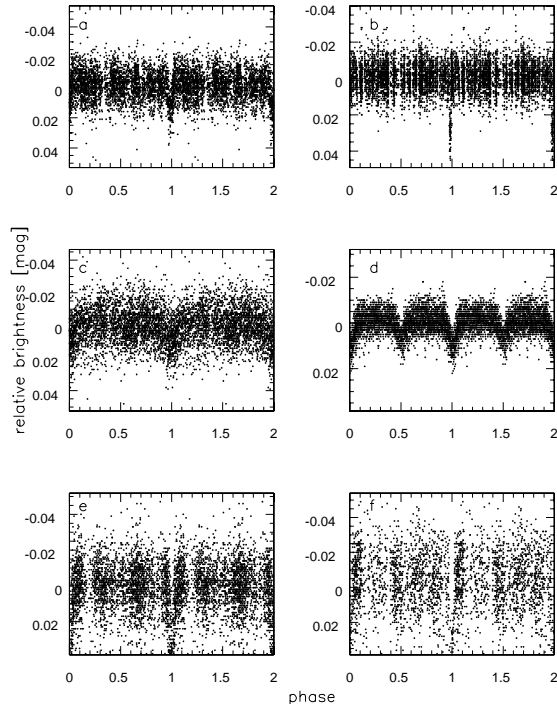


Fig. 1.— Exemplary light curves for XO astrophysical false positives. In all cases two cycles are shown and phase 0 corresponds to middle of the transit. Best ephemeris given in this paper were used. Data were calibrated using SysRem algorithm. Star designations: *a* – J0401..., *b* – J040022..., *c* – J0736..., *d* – J0745..., *e* – J23503..., *f* – J2351....

We identified only two objects listed in Table 1 in common with these lists: J00023... and J1157..., for which transits were found by SuperWASP project. These stars are described in more detail in §5. The reason for such a small number of common objects may result from different automated cutoff limits of calculated quantities, and the fact that the fraction of recovered transits does not equal unity for all periods under consideration. The observing window causes problems with revealing transits occurring at some periods, especially integer-day and long ones. Simulations show that the fields analyzed by Christian et al. (2006) were observed sufficiently to recover all transits shorter than 3 d. This is also true for half of the fields observed by Kane et al. (2008) and not

true for the analysis presented by Clarkson et al. (2007). Another similar lists were presented by O'Donovan et al. (2007), Street et al. (2007) and Lister et al. (2007) but their fields did not overlap the XO fields.

As marked in Table 1 some of astrophysical false positives have flat-bottomed transits (U-shape) and others have long ingress and egress with little or no “bottom” (V-shape). If ET observations exist they were used to assign U or V. The former (U-shaped) presumably are showing total eclipses and the latter (V-shaped) are on grazing incidence orbits. Because some of the U-shaped transits may be caused by eclipsing M dwarfs (or even brown dwarfs) they are good targets for additional follow-up observations.

#### 4. Radial Velocity measurements

Only a few of the XO candidates turned out to be planets (Burke et al. 2007, 2008; Johns-Krull et al. 2008; McCullough et al. 2006, 2008). Table 1 demonstrates the importance of the ET follow-up photometry to the XO project in order to keep the false positive rate for RV measurements low, as spectroscopic verification requires precious time on large telescopes. Scheduling RV measurements is straight forward because the RV is changing all the time, whereas the planetary transit reveals itself only for a few percent of the period. Sometimes two RVs show a difference much larger than  $1 \text{ km}\cdot\text{s}^{-1}$  (planets orbiting other stars typically show smaller RV amplitude) and prove the companion is not a planet. The advantage of taking spectra is more pronounced for long-period objects or ones with periods close to an integer number of days, e.g. OGLE-TR-111-b whose transits were unobservable from northern Chile in 2007 (Minniti et al. 2007).

Spectra were taken using spectrographs at: 2.7 m Harlan J. Smith Telescope (HJS) at McDonald Observatory, 4 m Nicholas U. Mayall Telescope at Kitt Peak National Observatory and 11 m Hobby-Eberly Telescope (HET) at McDonald Observatory. For detailed description of the spectrographs see Tull et al. (1995), the KPNO website<sup>2</sup> and Tull (1998), respectively. Exposure times were between 150 s and 1800 s. Typical

resolution ( $\lambda/\Delta\lambda$ ) was  $\approx 60,000$ .

In this work the astrophysical false positives that produce large ( $\gg 1 \text{ km}\cdot\text{s}^{-1}$ ) RV variation do not require the analysis used for planets (McCullough et al. 2006). Instead we applied less precise and simpler method. All the spectra had the wavelength solutions calculated using the ThAr arc lamp which was observed during each observing night. The spectra were cross-correlated using Tonry & Davis (1979) method with the solar spectrum (Kurucz et al. 1984). For HJS, Mayall and HET telescopes respectively, for each spectrum 11, 8 and 19 orders were usually used with average lengths of  $60\text{\AA}$ ,  $65\text{\AA}$  and  $59\text{\AA}$ . The main sources of the RV errors are: insufficiently accurate wavelength solution, the spectral type mismatch (see e.g. Nidever et al. 2002), and to a much smaller degree, convective blueshift and gravitational redshift.

Three stars (J00121..., J0813... and J1157...) showed evidence for large rotational broadening. For these stars telluric lines from H $\alpha$  region were removed and projected rotation speed of the star ( $v \sin i$ ) was found by minimizing  $\chi^2$  between the rotationally broaden solar template and the observed spectrum in H $\alpha$  region. This region was chosen because abundance of Hydrogen does not change as much as it does for other elements from star to star and it gave us many data points. It was repeated for every spectrum of a target star and results were averaged to obtain the final  $v \sin i$  estimation. For these 3 stars, we cross correlated their spectra with rotationally broaden solar template.

Some stars exhibit significant RV variations ( $\gg 1 \text{ km}\cdot\text{s}^{-1}$ ) and thus they were removed from the target list as stellar EBs. For most of them we had 1 or 2 observations from each of 2 different nights. We assumed our photometric ephemerides were correct and the orbits are circular. For some objects we give better ephemeris in notes for Table 1 and these are the ones used for the calculations. Then, the radial velocity ( $RV(t)$ ) measured at the time ( $t$ ) should follow the relation:

$$RV(t) = RV_0 - K \cdot \sin\left(\frac{t - T_0}{P} \cdot 2\pi\right) \quad (2)$$

which allowed us to estimate the values of semi-amplitude ( $K$ ) and systemic velocity ( $RV_0$ ). All of these systems show eclipses so  $i \approx 90^\circ$ . We used

<sup>2</sup><http://www.noao.edu/kpno/manuals/echman/>

the RV semi-amplitude  $K$  and the period to determine the mass function ( $f(m)$ ). An approximate mass estimate ( $m_{est}$ ) for the less massive companion follows if we assume its mass is much smaller than the mass of the primary ( $M$ ):

$$m_{est} = (f(m))^{1/3} M^{2/3} \quad (3)$$

To estimate  $M$  we used  $J-H$  colors from 2MASS, mass-colour relations from Drilling & Landolt (2000) and assumed the primary is a main sequence star. One should note these  $m_{est}$  are rough estimates done mainly for choosing targets for follow-up observations.

Table 2 gives the journal of RV measurements for stars with significant RV shift. Table 3 summarizes results for these binaries. We found no RV data for these systems in external databases (e.g. ADS and SIMBAD). For stars with exactly 2 RV measurements,  $K$  and  $RV_0$  were calculated directly and in all other cases we produced a least-squares estimate. For 2 targets (J00021... and J0007...) we were not able to fit a model (Equation 2) to the data, because each had a dubious period, considerable measurement uncertainty, or perhaps due to a non-circular orbit. For J2359... we found negative  $K$ , presumably due to an incorrect photometric period or phase. In both these cases we have estimated a lower limit of  $K$  as half of the difference between maximum and minimum  $RV(t)$ , and associated lower limits of  $f(m)$  and  $m_{est}$ , with the caveat that the latter depends on the period. There is small possibility that J2359... is a rare example of an EB with components of similar effective temperatures, an eccentric orbit, and the smaller star transiting the larger one, but the secondary eclipse is not observed due to the inclination.

We have revealed six new double line spectroscopic binaries namely: J03482..., J0722..., J0727..., J1511..., J1540... and J23565....

## 5. Notes on selected stars

**J00021...** The period is unreliable. We did not find one which fits well to our photometry and RVs. The egress is  $\approx 1$  h long and only 2 transits were observed (2452912.833 JD and 2453295.824 JD). A 22 d period was used to estimate  $f(m)$  and  $m_{est}$ .

**J00023...** This object was identified independently by Christian et al. (2006). Time of their epoch (taken with weight 3) and ET observation were used to refine the ephemeris for transit center:  $T_c = 2453653.7774 + E \cdot 2.37554$ . Christian et al. (2006) report a companion radius equal to  $2.07 R_J$ ; ours is  $2.4 R_J$ . Christian et al. (2006) also report a large ellipsoidal amplitude. There are two stars of similar brightness  $1''.2$  apart, thus probably one of them is an EB with twice larger amplitude demonstrating a stellar nature of the “transiting” object. The centroid shift method applied to the XO data is not sensitive to such small separations.

**J0015...** The brightest object within the XO photometric aperture is 2MASS J001524.05+325625.2 ( $J = 10.48$ ). We have found significant centroid shift in XO data at PA =  $339^\circ 5$ . The closest star with similar PA is 001523.09+325708.2 ( $J = 12.54$ , PA =  $344^\circ 4$  and  $d = 44''.7$ ), but another possibility is that 2MASS J001516.43+325849.4 ( $J = 10.67$ , PA =  $326^\circ 4$  and  $d = 173''.2$ ) causes observed variability.

**J040022...** The XO observed only 2 partial transits of this object, separated by 34 d. Both ingress and egress last  $\approx 3$  h. We observed a local minimum of RV with the Mayall telescope one season later than the latest XO photometry (see Figure 2). The ephemeris which fits all of our data,  $T_c = 2452964.12 + E \cdot 17.08$ , was used for calculations in Table 3. The  $B-V = 1.0$ , the eclipse is U-shaped with long ingress and egress. The best solution we have found it is a K giant orbited by a dwarf.

**J1157...** This candidate was identified independently by Kane et al. (2008). ET observations combined with XO survey data give the ephemeris:  $T_c = 2453436.1140 + E \cdot 2.45379$ . Our RV measurements show its eclipses are not caused by a planet because it exhibits  $30 \text{ km} \cdot \text{s}^{-1}$  shift in 1 d.

**J1515...** For this object one can see out of transit variations in XO data. Only two transits were observed and periods  $16.85488/i \text{ d}$  ( $i$  is an integer) are consistent with photometric data. Four RV measurements constrained the period. Best fitting

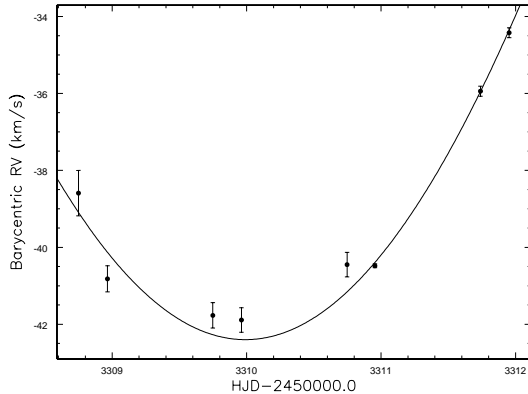


Fig. 2.— RV of J040022.... Line is defined by Equation 2 with parameters taken from Table 3 and ephemeris given in §5.

ephemeris is  $T_c = 2453866.0476 + E \cdot 5.61829$  and it was used to obtain values presented in Table 3.

**J1516...** We have observed only a few transit events for this star. The best observation showed egress beginning 2453878.95 JD and ending 2453880.10 JD. Thus egress lasts  $\approx 3.5$  h and the whole transit is  $\approx 27.5$  h (see Figure 3) so we interpret it as a long period system. The shortest time difference between transits observed by XO is  $\approx 26$  d, *i.e.* three times longer than value found using BLS. The fact that eclipses are observed implies inclination close to  $90^\circ$ . If we also assume mass of the primary star  $1M_\odot$  than the crude estimate (Eq. 2 McCullough et al. 2006) of the stellar radius is  $6R_\odot$ . It depends on period assumed: a period of 50 d gives half the former radius. We assign this candidate to be a giant orbited by a main sequence star.

## 6. Conclusions

This paper presents list of 69 stars with light curves that mimic planetary transits but the follow-up investigation demonstrated they are instead astrophysical false positives: grazing-incidence orbits of EBs, eclipses of a large star by an M dwarf, or eclipsing systems whose light has been diluted by a nearby bright star. Fifteen light curves were classified as V-shape and fifteen as U-shape. The list can be helpful for others searching for transiting planets, and also for eclipsing

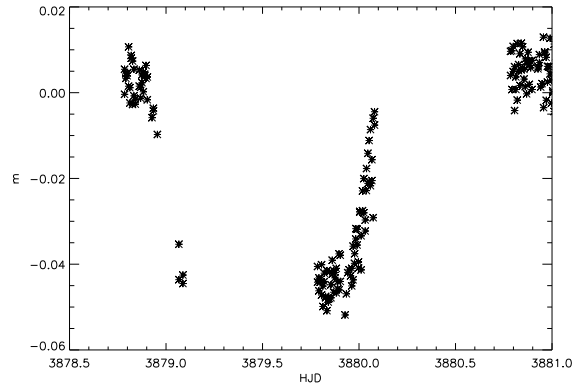


Fig. 3.— XO light curve for 3 nights of J1516.... Data were calibrated using SysRem algorithm. Size of points does not indicate errors. 0 mag corresponds to mean brightness.

binaries, with low-mass stellar companions.

Most of the stars in Table 1 are located in the strips centered at 0 and 4 hours RA. Those strips were the first to be observed. With greater experience, our improved algorithms (McCullough & Burke 2007) produced a smaller number of astrophysical false positives from other strips. Transit depths found by the BLS algorithm range from 4 mmag to 69 mmag. In Figure 4 we present histogram of periods presented in Table 1. Most of astrophysical false positives have periods shorter than 3.5 d. Obviously, probability of detecting short lasting events like transits is lower for longer period objects.

RVs presented in this paper have typically uncertainties of 400 m/s. For 15 single-line spectroscopic binaries we have estimated mass function. Six new double-line spectroscopic binaries were revealed. Additional remarks for some objects were given.

The most interesting objects for follow-up observations, which aim is to find low-mass secondaries of EBs, are systems with the smallest value of mass function given in Table 3. Among the stars without RV measurements the ones with the smallest transit depths and U-shaped eclipses should be the most promising.

R. P. is grateful to the AURA for the Summer Student Program at STScI as well as I.

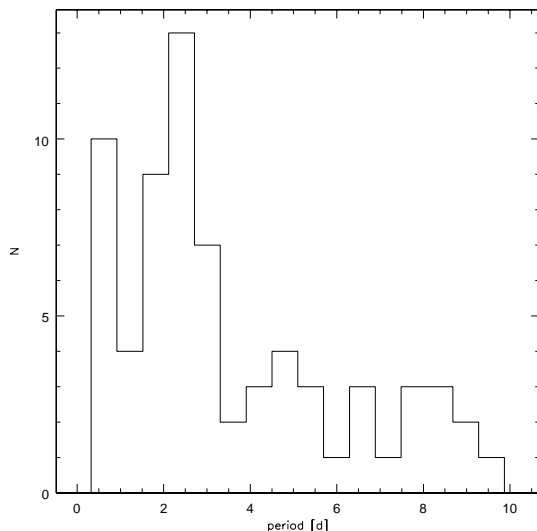


Fig. 4.— Histogram of periods presented in Table 1.

Soszyński for comments on manuscript. This publication makes use of catalogs VizieR and SIMBAD operated at CDS, Strasbourg, France, and data products from the 2MASS, which is a joint project of the University of Massachusetts and the IPAC/Caltech, funded by the NASA and NSF.

## REFERENCES

- Bakos, G. Á., Lázár, J., Papp, I., Sári, P., & Green, E. M. 2002, *PASP*, 114, 974
- Beatty, T. G. et al. 2007, *ApJ*, 663, 573
- Burke, C. J., Gaudi, B. S., DePoy, D. L., & Pogge, R. W. 2006, *AJ*, 132, 210
- Burke, C. J. et al. 2007, *ApJ*, 671, 2115
- Burke, C. J. et al. 2008, *ApJ*, 686, 1331
- Brown, T. 2003, *ApJ*, 593, L125
- Charbonneau, D., Brown, T. M., Burrows, A., & Laughlin, G. 2007, in *Protostars and Planets V*, ed. B. Reipurth, D. Jewitt, & K. Keil, (Tucson: Univ. Arizona Press), 701, preprint (astro-ph/0603376)
- Christian, D. J. et al. 2006, *MNRAS*, 372, 1117
- Clarkson, W. I. et al. 2007, *MNRAS*, 381, 851
- Couteau, P. 1983, *A&ASS*, 53, 441
- Creevey, O. L. et al. 2005, *ApJ*, 625, L127
- Dommanget, J., & Nys, O. 2002, *Obs. et Travaux*, 54, 5
- Drilling, J. S., & Landolt, A. U. 2000, in *Allen's Astrophysical Quantities*, ed. A. N. Cox (New York: Springer-Verlag), 381
- Dunham, E. W., Mandushev, G. I., & Taylor, B. Q. 2004, *PASP*, 116, 1072
- Fabrizius, C., Høg, E., Makarov, V. V., Mason, D. B., Wycoff, G. L., & Urban, S. E. 2002, *A&A*, 384, 180
- Garcia-Melendo, E., & McCullough, P. R. 2009, *ApJ*, 698, 558
- Hoyer, S. et al. 2007, *ApJ*, 669, 1345
- Johns-Krull, C. M. et al. 2008, *ApJ*, 677, 657
- Kane, S. R. et al. 2008, *MNRAS*, 384, 1097
- Kovács, G., Zucker, S., & Mazeh, T. 2002, *A&A*, 391, 369
- Kurucz, R. L., Furenlid, I., Brault, J., & Testerman, L. 1984, *National Solar Observatory Atlas No. 1: Solar Flux Atlas from 296 to 1300 nm* (Sunspot: NSO)
- Lister, T. A. et al. 2007, *MNRAS*, 379, 647
- McCullough, P. R., Stys, J. E., Valenti, J. A., Fleming, S. W., Janes, K. A., & Heasley, J. N. 2005, *PASP*, 117, 783
- McCullough, P. R. et al. 2006, *ApJ*, 648, 1228
- McCullough, P. R. & Burke, C. J. 2007, *ASP Conf. Ser., Transiting Extrasolar Planets Workshop*, ed. C. Afonso, D. Weldrake, & T. Henning (San Francisco: ASP), preprint (astro-ph/0703331)
- McCullough, P. R. 2008, *ApJ*, submitted, preprint (astro-ph/0805.2921)
- Minniti, D. et al. 2007, *ApJ*, 660, 858
- Nidever, D., Marcy, G., Butler, R., Fischer, D., & Vogt, S. 2002, *ApJS*, 141, 503
- O'Donovan, F. T. et al. 2007, *ApJ*, 662, 658

- Paczynski, B. 2000 PASP, 112, 1281
- Pollacco, D. et al. 2006, PASP, 118, 1407
- Skrutskie, M. F. et al. 2006, AJ, 131, 1163
- Street, R. A. et al. 2007, MNRAS, 379, 816
- Tamuz, O., Mazeh, T., & Zucker, S. 2005, MNRAS, 356, 1466
- Tonry, J., & Davies, M. 1979, AJ, 84, 1511
- Tull, R. G., MacQueen, P. J., Sneden, C., & Lambert, D. L. 1995, PASP, 107, 251
- Tull, R. G. 1998, Proc. SPIE, 3355, 387
- Young, T. B., Hidas, M. G., Webb, J. K., Ashley, M. C. B., Christiansen, J. L., Derekas, A., & Nutto, C. 2006, MNRAS, 370, 1529



TABLE 1  
ASTROPHYSICAL FALSE POSITIVES FOUND BY X0

2MASS	$m_{XO}$ (mag)	FL75	$\delta m$ (mag)	$\delta m_{FL75}$ (mag)	$t_{dur}$ (h)	P (d)	$T_0$ JD-2450000.0	Flags
<i>J000210.00+474803.6</i>	10.98	0.93	0.011	0.012	3.68	9.57487	3295.817	SB1
<i>J000233.06+331517.3</i>	10.96	0.47	0.022	0.047	1.82	2.37552	3653.765	V
J000629.13+355242.4	9.84	0.08	0.004	0.052	1.46	0.897843	3319.745	...
J000744.08+402835.4 <sup>a</sup>	10.17	0.93	0.015	0.016	2.19	2.84981	2948.804	SB1
J000857.97+025642.0 <sup>b</sup>	10.12	1.00	0.011	0.011	3.17	4.72277	3653.778	SB1
J001215.64+335112.1	11.33	0.96	0.011	0.012	3.14	6.55222	3295.906	SB1
J001222.06+142422.6 <sup>c</sup>	12.08	0.96	0.050	0.053	2.06	1.07386	3287.018	V
J001446.58+301646.2 <sup>d</sup>	9.39	0.86	0.042	0.048	1.87	2.16132	3318.841	U
<i>J001523.09+325708.2</i>	11.56	0.15	0.036	0.261	2.58	1.79057	3320.819	P&S, V
J033955.56+452329.5	9.43	0.95	0.017	0.018	3.37	8.77347	3322.084	SB1
J034610.90+283212.5	10.57	0.22	0.017	0.080	2.81	4.87377	3300.980	SB1, V
J034829.26+052719.5	11.23	0.94	0.021	0.022	3.50	4.56329	3328.900	SB2
J034854.48+420725.0 <sup>e</sup>	10.41	0.97	0.031	0.032	3.40	3.22290	3312.044	V
J035046.19+454253.9	11.49	0.06	0.015	0.253	3.05	1.67403	3369.903	V
J035129.86+460956.8 <sup>f</sup>	11.83	0.61	0.069	0.115	3.64	7.59071	3350.973	U
J035215.14+545101.3 <sup>g</sup>	12.09	0.19	0.021	0.119	3.14	4.67552	3351.941	...
J035308.94+053633.1	10.98	1.00	0.015	0.015	3.29	6.86153	3356.835	SB1, U
J035403.37+150830.3	9.04	0.98	0.024	0.025	2.07	7.19632	3657.953	SB1
J035635.76+274551.0	11.69	0.51	0.031	0.061	2.31	2.67151	3375.746	P&S, V
J035747.56+341415.4	11.28	0.06	0.022	0.413	2.89	1.67034	3376-788	V
J035839.54+071617.8 <sup>h</sup>	11.26	0.01	0.016	...	3.18	2.20751	3323.031	...
J035931.11+011806.1 <sup>i</sup>	11.99	0.99	0.010	0.010	1.28	0.782130	3654.135	...
J035954.57+424555.7 <sup>j</sup>	10.82	0.48	0.023	0.047	3.77	7.86040	3652.139	...
J040016.44+540120.3	10.62	0.92	0.039	0.042	2.24	1.94803	3322.124	P&S, V
J040025.10+022526.6 <sup>k</sup>	11.34	0.13	0.016	0.127	3.33	5.77968	3376.784	...
<i>J040022.90+090533.6</i>	11.32	1.00	0.028	0.028	3.29	8.51064	2997.898	SB1, U
J040052.03+532245.9 <sup>l</sup>	9.42	0.44	0.019	0.044	3.26	2.12368	3342.858	P&S, V
J040117.74+492843.0	10.72	0.80	0.037	0.047	3.34	8.70322	3375.779	P&S
J040425.98+480532.2	12.00	0.10	0.018	0.199	2.42	1.57639	3321.955	...
J040559.26+512758.7	11.47	0.32	0.012	0.039	1.85	0.622076	3658.103	V
J040905.12+180323.7	12.16	0.28	0.016	0.059	2.54	1.55560	3348.984	V
J040919.39+485819.3	12.25	0.14	0.047	0.394	2.20	1.62185	3293.096	...
J041114.76+145420.9	11.77	0.23	0.015	0.068	3.19	2.21474	3350.764	V
J041144.50+311726.1	10.99	0.55	0.044	0.081	2.91	3.03067	3349.022	U
J041314.80+530431.9	10.74	0.12	0.011	0.089	3.22	4.19252	3369.894	...
J041326.43+443227.7 <sup>m</sup>	10.63	0.92	0.013	0.015	3.30	2.64145	3655.061	U
J041807.44+590552.7 <sup>n</sup>	9.80	0.87	0.030	0.035	1.46	3.04952	3658.079	...
J072222.81+255627.1	10.81	0.99	0.014	0.014	1.49	2.22311	4153.780	SB2
J072706.06+311708.9 <sup>o</sup>	9.85	0.75	0.016	0.022	3.57	4.12712	4152.766	SB2, U
J073625.33+614626.3	11.95	0.04	0.007	0.184	2.23	0.775711	3409.817	...
J074506.62+444650.6 <sup>p</sup>	9.83	0.03	0.007	0.269	1.82	0.860526	3398.780	V
J074943.04+005230.3	10.66	0.08	0.007	0.081	2.92	1.26759	3417.806	...
J080856.73+214452.8	10.24	0.96	0.025	0.026	2.99	5.19481	3412.027	SB1, U

TABLE 1—*Continued*

2MASS	$m_{XO}$ (mag)	FL75	$\delta m$ (mag)	$\delta m_{FL75}$ (mag)	$t_{dur}$ (h)	P (d)	$T_0$ JD-2450000.0	Flags
J081137.72+212013.8 <sup>q</sup>	10.85	0.05	0.017	0.376	2.34	2.44248	3419.821	V
J081338.69+372352.4 <sup>r</sup>	11.95	0.50	0.009	0.017	1.82	2.71400	3436.794	SB1, V
J114634.97+544538.8	11.96	0.83	0.017	0.021	2.05	3.56608	3491.831	V
<i>J115718.68+261906.1</i>	11.10	0.89	0.013	0.015	2.59	2.45387	3436.114	SB1, U
J151110.13+385703.1 <sup>s</sup>	8.96	1.00	0.021	0.021	1.88	1.50525	4206.083	SB2, V
<i>J151559.79+503139.4</i>	10.77	0.99	0.018	0.018	3.23	8.42744	3866.048	SB1
<i>J151623.71+090139.2</i>	10.27	0.97	0.045	0.047	4.93	8.55725	3879.850	U
J151843.24+533338.8SW <sup>t</sup>	9.66	1.00	0.025	0.025	3.28	3.79276	4221.107	SB1, U
J152327.59+023329.6	9.65	0.02	0.007	0.641	1.78	0.883986	4234.964	...
J153248.92+070945.1	11.94	0.12	0.018	0.166	1.24	0.807637	4200.965	...
J154046.82+621339.6	12.01	0.98	0.020	0.020	2.08	3.09962	3884.971	SB2
J155618.13+074537.6	11.97	0.05	0.010	0.236	3.21	2.39173	3506.011	...
J234031.68+474558.6	11.01	0.14	0.006	0.043	2.05	0.713328	3283.938	...
J234512.08+343544.5 <sup>u</sup>	12.45	0.85	0.037	0.043	2.44	6.35001	3293.848	...
J234822.41+185717.4 <sup>v</sup>	12.38	0.75	0.067	0.091	3.02	5.24164	3652.862	V
J234837.19+181348.7	9.79	0.97	0.041	0.042	3.75	7.81983	3665.835	P&S, U
J234959.04+311203.5	11.88	0.14	0.017	0.130	2.70	1.48091	3241.953	...
J235035.06+294350.3	12.04	0.85	0.025	0.030	3.38	2.93582	3650.769	P&S, V
J235048.78+440127.2 <sup>w</sup>	11.61	0.92	0.022	0.024	1.33	0.815248	3319.738	V
J235104.27+251629.3 <sup>x</sup>	12.40	0.53	0.030	0.058	2.43	2.53075	2912.854	U
J235219.65+434323.4	11.82	0.15	0.018	0.127	1.65	0.659657	3295.857	...
J235227.06+395515.1	11.87	0.02	0.008	0.391	2.94	1.53116	3321.854	...
J235602.52+415451.5	11.75	0.71	0.033	0.046	2.70	2.16572	3652.945	P&S, U
J235613.98+402648.3 <sup>y</sup>	12.20	0.55	0.022	0.040	2.54	4.41618	3318.862	P&S
J235650.15+160754.7	12.15	0.88	0.039	0.045	2.60	1.59084	3651.045	SB2, U
J235929.73+444031.2	10.61	0.97	0.032	0.033	3.27	5.68117	3320.788	SB1, U

NOTE.—Astrophysical false positives found by the X0 project. Additional comments for stars marked by italics can be found in Section 5. The flags are: (P&S) — evidence for different primary and secondary minima if the light curve is folded with double period, (SB1) — spectroscopic single line binary, (SB2) — spectroscopic double line binary, (U) — transit is U-shaped, (V) — transit is V-shaped.

<sup>a</sup>The Period is  $39.897/i$  where  $i = 1, 2, 3, 6, 7, 14$  and  $i = 14$  seems most probable.

<sup>b</sup>Only 2 transits 344.02 d apart were observed with different depths.

<sup>c</sup>The XO amplitude is 0.07 mag and it is too big for a planetary transit.

<sup>d</sup>The ET measured the  $R$  amplitude 0.065 mag which is too big for a planetary transit.

<sup>e</sup>The  $R$  amplitude  $\geq 0.07$  mag and the transit lasts at least 6 h, so it is too deep and too long for a planetary transit.

<sup>f</sup>ET observations showed the  $R$  amplitude  $\geq 0.11$  mag and were used to find better ephemeris:  $T_c = 2453550.9416 + E \cdot 7.58945$ .

<sup>g</sup>The ET observations showed it is an EB with different depths and half period. The ephemeris is:  $T_c = 2453351.9538 + E \cdot 2.33781$ .

<sup>h</sup> $\delta m_{FL75}$  is smaller than  $\delta m$ . It shows our estimation of photometric aperture is not working well in this case. ET found  $R$  amplitude  $\geq 0.80$  mag.

<sup>i</sup>Secondary eclipses were observed by the XO.

<sup>j</sup>The ET found  $R$  amplitude  $\geq 0.058$  mag. There is a bright stars nearby. The ingress and the egress lasts  $\approx 2$  h each. Most probable periods are 15.7191 d and 7.8595 d.

<sup>k</sup>If double period is used than out of transit variation is seen on the XO data. There is brighter nearby star 2MASS J040026.26+022555.7 and centroid shift was found at PA =  $239^\circ 0$ . The star 040025.10+022526.6 is situated  $d = 34''.7$  apart at PA =  $237^\circ 0$ .

<sup>l</sup>Fabricius et al. (2002) found this is a visual binary and gave it designation TDSC 8509. The brighter component is 2MASS J040049.67+532237.3. Centroid shift was found in XO data at PA =  $17^\circ 2$ . We revealed TDSC 8509 B (2MASS J040052.03+532245.9) to be a binary system itself. It is located  $d = 36''.4$  apart at PA =  $13^\circ 7$ .

<sup>m</sup>If we assume this star to have Jupiter size planet than given period gives us estimation of transit length of  $\approx 1.9$  h and length measured on the XO data is too long. ET show even longer event lasting  $\approx 4$  h.

<sup>n</sup>The XO observed only two ingresses which are separated by 365.91 d and last  $\approx 1.5$  h. This object has definitely a very deep eclipses and probably period of few times longer than 3.05 d.

<sup>o</sup>This is known double star TDSC 19502 Fabricius et al. (2002).

<sup>p</sup>The ET found filter-dependent amplitudes: 0.47 mag in  $B$ , 0.40 mag in  $V$ , 0.35 mag in  $I$  and 0.40 mag in  $R$ . Primary and secondary minima are observed.

<sup>q</sup>Better ephemeris was found using the ET observations:  $T_c = 2453419.8112 + E \cdot 2.44269$ .

<sup>r</sup>Better ephemeris was found using the ET observations:  $T_c = 2453436.7858 + E \cdot 2.71387$ .

<sup>s</sup>Shows different depth transits when phased with four times longer period. Out of transit variation is observed.

<sup>t</sup>This is known double star. It has one designation in 2MASS thus FL75 is 1.0, but should be  $\approx 0.5$ . We are designating components: 151843.24+533338.8SW (CCDM15187+5334A) and 151843.24+533338.8NE (CCDM15187+5334B). See Dommanget & Nys (2002) for more information.

<sup>u</sup>The ET observations show the transit at least 0.05 mag deep so companion is thus at least  $2R_J$  what is too big for a planet.

<sup>v</sup>The XO amplitude is 0.09 mag.

<sup>w</sup>The ET found filter-dependent amplitudes: 0.02 mag in  $B$ , 0.03 mag in  $V$  and 0.04 mag in  $R$ .

<sup>x</sup>The ET found that  $R$  amplitude is 0.07 mag.

<sup>y</sup>The Period is dubious (may be even 5 times longer) because only 1 ingress and 2 egresses were observed. The XO amplitude is 0.03 mag. The ET found  $R$  and  $V$  amplitudes are 0.04 mag and transit duration is at least 3 h.

TABLE 2  
RV MEASUREMENTS FOR EBS

2MASS designation	$t$ (HJD-2450000.0)	Telescope	$RV(t)$ (km·s <sup>-1</sup> )	$\sigma_{RV}$ (km·s <sup>-1</sup> )
J00021. . .	3308.6305	Mayall	-1.18	0.14
J00021. . .	3309.6245	Mayall	-1.65	0.33
J00021. . .	3310.6160	Mayall	-3.92	0.12
J00021. . .	3310.8680	Mayall	-4.84	0.13
J00021. . .	3311.6177	Mayall	-6.10	0.22
J00021. . .	3954.7807	HET	-27.28	0.12
J00021. . .	3954.7845	HET	-27.54	0.27
J00021. . .	3958.8006	HET	-22.57	0.06
J00021. . .	3958.8044	HET	-22.58	0.08
J00021. . .	3965.7672	HET	-1.90	0.21
J00021. . .	3965.7709	HET	-1.88	0.23
J0007. . .	3308.6537	Mayall	-23.56	0.30
J0007. . .	3308.8803	Mayall	-25.83	0.15
J0007. . .	3309.6477	Mayall	-29.88	0.06
J0007. . .	3309.8735	Mayall	-31.72	0.17
J0007. . .	4321.8032	HET	-4.81	0.17
J0007. . .	4322.7790	HET	-6.47	0.10
J0008. . .	3308.7077	Mayall	8.03	0.21
J0008. . .	3308.8137	Mayall	5.21	0.20
J0008. . .	3309.7035	Mayall	-6.26	0.31
J0008. . .	3309.8146	Mayall	-8.40	0.15
J00121. . .	4309.8301	HET	-0.7	5.6
J00121. . .	4318.8004	HET	-33.9	2.8
J0339. . .	3997.8284	HET	-25.0	1.7
J0339. . .	4003.8122	HET	-8.7	2.1
J0346. . .	3310.7882	Mayall	-1.11	0.77
J0346. . .	3311.8722	Mayall	-42.45	0.17
J0353. . .	3308.7732	Mayall	-29.86	0.53
J0353. . .	3308.9357	Mayall	-32.01	0.27
J0353. . .	3309.7733	Mayall	-42.43	0.37
J0353. . .	3309.9330	Mayall	-43.05	0.24
J0354. . .	3997.8496	HET	-29.99	0.07
J0354. . .	4001.8444	HET	6.55	0.17
J040022. . .	3308.7492	Mayall	-38.59	0.59
J040022. . .	3308.9650	Mayall	-40.82	0.34
J040022. . .	3309.7484	Mayall	-41.77	0.33
J040022. . .	3309.9615	Mayall	-41.89	0.32
J040022. . .	3310.7467	Mayall	-40.45	0.32
J040022. . .	3310.9537	Mayall	-40.48	0.05
J040022. . .	3311.7390	Mayall	-35.94	0.13
J040022. . .	3311.9523	Mayall	-34.42	0.13
J0808. . .	4141.8338	HJS	48.04	0.32
J0808. . .	4142.8604	HJS	61.19	0.51
J0808. . .	4143.8531	HJS	56.84	0.83

TABLE 2—*Continued*

2MASS designation	$t$ (HJD-2450000.0)	Telescope	$RV(t)$ (km·s <sup>-1</sup> )	$\sigma_{RV}$ (km·s <sup>-1</sup> )
J0813...	4140.9303	HJS	-24.8	1.7
J0813...	4178.7487	HET	-39.6	1.1
J0813...	4179.7464	HET	21.9	1.5
J1157...	4225.7663	HET	23.32	0.78
J1157...	4226.7732	HET	-8.67	0.45
J1515...	4141.0176	HJS	20.42	0.26
J1515...	4141.9549	HJS	-30.58	0.30
J1515...	4142.9524	HJS	-42.41	0.88
J1515...	4144.9652	HJS	45.15	0.35
J1518...	4139.0004	HJS	-69.89	0.27
J1518...	4140.9836	HJS	-28.24	0.17
J1518...	4141.9675	HJS	-68.20	0.22
J1518...	4142.9678	HJS	-64.36	0.60
J2359...	3310.6391	Mayall	-19.07	0.42
J2359...	3311.7990	Mayall	-26.36	0.50

NOTE.—RV measurements for EBs. See §4 for description of weights and data reduction.

TABLE 3  
RV PARAMETERS FOR EBs

2MASS designation	$v \sin i$ (km·s <sup>-1</sup> )	$K$ (km·s <sup>-1</sup> )	$RV_0$ (km·s <sup>-1</sup> )	$f(m)$ ( $M_\odot$ )	$M$ ( $M_\odot$ )	$m_{est}$ ( $M_\odot$ )
<i>J00021...</i>	...	$\geq 13.10$	...	$\geq 0.0051$	1.3	$\geq 0.17$
J0007...	...	$\geq 13.12$	...	$\geq 0.00067$	1.4	$\geq 0.087$
J0008...	...	12.39	2.68	0.00093	1.5	0.13
J00121...	56.5±0.5	20.31	-21.01	0.0057	1.5	0.23
J0339...	...	15.20	-23.16	0.0032	1.5	0.19
J0346...	...	45.05	2.39	0.046	1.0	0.36
J0353...	...	15.12	-30.22	0.0025	1.3	0.16
J0354...	...	18.57	-11.56	0.0048	1.4	0.21
<i>J040022...</i>	...	32.29	-10.11	0.060	0.9	0.36
...	...	...	...	...	1.0	0.39
J0808...	...	12.59	49.30	0.0011	1.6	0.14
J0813...	39.9±1.0	37.31	-15.22	0.015	1.4	0.31
<i>J1157...</i>	40.1±2.0	16.66	7.47	0.0012	1.5	0.14
<i>J1515...</i>	...	52.28	2.49	0.083	1.5	0.57
J1518...	...	27.56	-47.70	0.0082	1.0	0.20
J2359...	...	-15.22	-33.90	$\geq 0.000029$	1.4	$\geq 0.031$

NOTE.—RV parameters for EBs. See §4 for description of analysis and §5 for comments concerning stars marked by italics. For J040022... two estimates are given. For first one we have assumed its luminosity class is V, for second – class III.